Isı Bilimi ve Tekniği Dergisi, 33, 1, 55-61, 2013
J. of Thermal Science and Technology

ISSN 1300-3615

EXPERIMENT AND SIMULATION TO DEVELOP CLEAN POROUS MEDIUM SURFACE COMBUSTOR USING LPG

Musthafa ABDUL MUJEEBU*,, Mohammad Zulkifly ABDULLAH* and Mohammed ZUBER***

* Universiti Sains Malaysia, School of Mechanical and Aerospace Engineering, Porous Media Combustion Laboratory, Engineering campus, 14300 Nibong Tebal, Penang, Malaysia
mamujeeb5@yahoo.com, Phone: 0060143051476
**Department of Mechanical Engineering, Anjuman Institute of Technology and Management, 581320 Bhatkal, Karnataka, India

(Geliş Tarihi :09.06.2011 Kabul Tarihi:21.09.2011)

Abstract: This paper presents the development, charcterization and numerical simulation of compact premixed LPG burner based on surface combustion in porous inert medium. The preheating and reaction zones are made up of Alumina (Al_2O_3) foams of pore sizes 26 ppcm and 8 ppcm, respectively. Experiments are conducted with 0.45 litres per minute (lpm) of LPG fuel, which is found to be the minimum quantity required to produce a sustainable flame when mixed with 4 lpm of air. The temperature distribution within the combustor, flame stability, maximum flame temperature, NO, CO and SO_2 emissions and thermal efficiency are measured and compared with those of conventional LPG stove. It is found that the proposed burner could yield 80% saving in fuel consumption and 75% reduction in NOx emission compared to the conventional one. The CO and SO_2 emissions are also within the permissible limits. The thermal efficiency is estimated to be 71% whereas for the conventional burner is 47%, for a thermal load of 0.62 kW. Effects of porosity and thickness of reaction layer are studied by means of a two dimensional simulation using FLUENT software, considering single step reaction and thermal equilibrium between phases. Experimental and numerical findings are found in satisfactory agreement.
Keywords: Porous medium; Surface combustion; Emission; Thermal efficiency.

LPG KULLANAN TEMİZ GÖZENEKLİ ORTAM YÜZEY YAKICISI DENEYİ VE SİMÜLASYONU

Özet: Bu çalışmada, kompakt yüzeyde yanma temelli ön karışımlı LPG yakıcısının geliştirilmesi, karakteristiklerinin belirlenmesi ve sayısal simülasyonu verilmiştir. Ön ısıtma ve reaksiyon bölgeleri sırası ile 26 ppcm ve 8 ppcm gözenek çaplı alumina (Al_2O_3) köpükten imal edilmiştir. Deneyler 4 litre/dakika debideki hava ile karışım yaparak, sürekli yanmayı sağlayabilmek için gerekli olan en az miktar 0.45 litre/dakika LPG ile gerçekleştirilmiştir. Yanma odası içerisindeki sıcaklık dağılımı, alev stabilitesi, en yüksek alev sıcaklığı, NO, CO ve SO_2 emisyonları ve ısıl verim ölçülmüş ve konvansiyonel LPG fırını ile kıyaslanmıştır. Konvansiyonel yakıcı ile kıyaslandığında, önerilen yakıcı % 80 yakıt tasarrufu ve % 75 NO_x emisyonlarında azalma sağladığı görülmüştür. CO ve SO_2 emisyonları izin verilen sınırlar içerisindedir. 0.62 kW ısıl yük için ısıl verim % 71 olarak belirlenmiştir. Bu yük için konvansiyonel yakıcı ısıl verim % 47'dir. Gözenekliliğin ve reaksiyon tabakası kalınlığının etkileri, FLUENT yazılımı kullanılarak, tek basamaklı reaksiyonun ve fazlar arasında ısıl dengenin dikkate alındığı iki boyutlu simülasyon ile incelenmiştir. Deneysel ve sayısal bulgular tatmin edici uyum içerisindedirler.
Anahtar Kelimeler: Gözenekli ortam; Yüzey yanması; Emisyon; Isıl verim.

INTRODUCTION

Porous Medium Combustion (PMC) has interesting advantages compared with free flame combustion due to the higher burning rates, the increased power dynamic range, the extension of the lean flammability limits and the low emissions of pollutants. This technology has become the focus of many researchers for the last few decades and substantial works, both numerical and experimental have been carried out; for more details see ref. (Mujeebu et al., 2009a; 2009b). Bone (1912), Luke (1913) and Hays (1933) were the pioneers of surface combustion in porous media. Later on, many researchers have focused on various problems related to this topic (Hanamura and Echigo, 1991; Williams et al., 1992; Nakamura *et al*., 1993; Bouma *et al*., 1995; Lammers and de Goey, 1995; Jugjai and Sawananon, 2004; Nemoda, 2004; Marbach *et al.*, 2005 & 2007). However, there is significant scope to develop energy efficient and eco-friendly burners using surface

combustion in porous medium (PM). In the current study a mesoscale, premixed PM burner (PMB), suitable for normal household applications, is developed. Double layer porous alumina foam with varying pore size is employed. The premixing is done in two stages, first in a swirler, then in a wire-mesh packing. The PMB is tested for its maximum flame temperature, thermal efficiency and emission characteristics compared to the conventional liquefied petroleum gas (LPG) burner (CB). A two dimensional simulation using FLUENT is also performed to observe the effect of porosity and thickness of reaction layer.

EXPERIMENTAL SETUP AND PROCEDURE

The schematic of the experimental porous surface burner is shown in Figure 1. The PM is made up of two layers of Alumina foam (Goodfellow Cambridge Limited, England), the bottom layer (12.7mm, 26ppcm, porosity 86%) forming the preheating zone and the top layer (12.7mm, 8ppcm, porosity 84%), the reaction zone. The premixer 1 is a swirler and premixer 2 is cylindrical steel wire-mesh packing of 30 cm length and 8cm diameter. K-type thermocouples (TC1 to TC5) are arranged along the axial direction of the burner to measure the temperatures at different locations as shown. The thermocouples are connected to the computer display through an 8- channel data logger (Pico Technology Limited, UK). The exhaust gas is collected at the top and analyzed by means of a high precision, portable gas analyzer (Draeger MSI Compact – NT, Germany) which gives direct values of CO NO_x and SO_2 in ppm (parts per million). The burner is operated with an excess air ratio of around 2, the velocity of the premixed air and fuel entering the burner is 0.89 m/s which is observed to be the minimum velocity to maintain a stable flame at the surface of the PM. In order to arrive at the best PM configuration various trials are made by changing the number and type of reaction layer.

The experiment is started by manually igniting the air fuel mixture, and the temperatures are recorded, until steady state is reached. After each 10 min, the emission emissions of CO, NOx etc. are recorded. Similar tests are conducted on the CB as well. To ensure accuracy, the experiments are repeated 3 to 4 times and errors are estimated by uncertainty analysis as proposed by Taylor (1997).

The thermal efficiency of the burners (η_{th}) is determined as:

$$\eta_{th} = \frac{Q_{useful}}{Qin} * 100\ \% \quad (1)$$

where

$$Q_{useful} = \left(m_w\, C_{pw} + m_c\, C_{pc}\right)(80 - T_{wi}) \div t \text{ kW} \quad (2)$$

$$Q_{in} = m_f CV \text{ kW} \quad (3)$$

Q_{in} is the energy input to the burner, m_f is the mass flow rate of fuel in kg/s, and CV is the calorific value of LPG. Q_{useful} is the sensible heat absorbed by a fixed quantity of water (m_w) and the container of mass m_c to raise the temperature from an initial value (T_{wi}) to 80°C which is chosen arbitrarily. So, Q_{useful} can be obtained by knowing the time taken (t) in seconds for heating and assuming suitable value for the heat capacities of water (C_{pw}) and the container (C_{pc}).

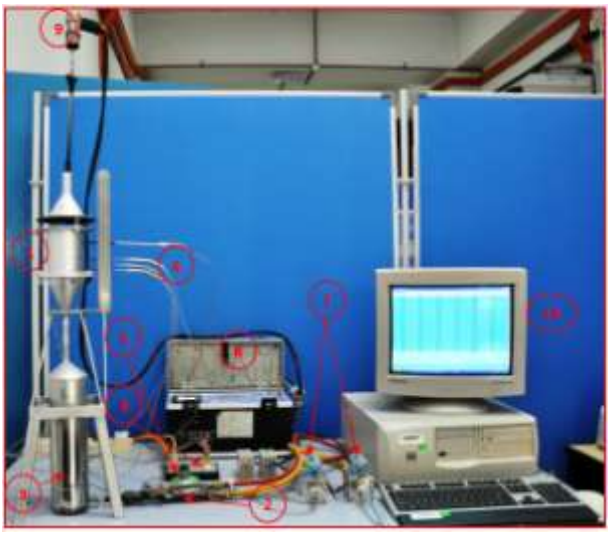

1. Burner main body, 2. Pre-mixer 1, 3. Pre-mixer 2,
4. Thermocouples, 5. Pressure reducing valve,
6. Data logger, 7. Digital flow meters, 8. Gas analyzer, 9. Gas analyzer probe, and 10. PC display.

Figure 1. The experimental setup.

NUMERICAL SIMULATION

Mathematical Model

A two dimensional steady state model with basic assumptions of equilibrium between phases (one-temperature model) and single step reaction (with six species) kinetics is considered. For the flow, viscous *k-ε* turbulence model with standard wall functions, no slip boundary conditions, species transport and finite-rate/eddy dissipation are assumed. Heat loss to the surrounding atmosphere through the wall is neglected. The basic governing equations are as follows.

Energy equation

FLUENT solves the energy equation in the following form:

$$\nabla.[\vec{v}(\rho E + p)] = \nabla.\left[k_{eff}\nabla T - \sum_j h_j \vec{J}_j + \left(\bar{\bar{\tau}}_{eff}.\vec{v}\right)\right] + S_h \quad (4)$$

where k_{eff} is the effective conductivity (k+ k_t), where k_t is the turbulent thermal conductivity, defined according to the turbulence model being used), and $\vec{J}_j$ is the diffusion flux of species j. The first three terms on the right-hand side of Eq. (4) represent energy transfer due to conduction, species diffusion and viscous dissipation respectively; and S_h incorporates the heat of chemical reaction, which also includes the source of energy due to chemical reaction:

$$S_h = -\sum_j \frac{h_j^o}{M_j} R_j \quad (5)$$

where h_j^o and R_j respectively are enthalpy of formation and volumetric rate of creation of species *j*.

Treatment of the energy equation in PM
For the PM region, Eq. (4) is modified by considering effective conductivity in the conduction flux:

$$\nabla.\left[\vec{v}(\rho_f E_f + p)\right] = \nabla.\left[k_{eff,pm}\nabla T - (\sum_i h_i J_i) + \tau.v + Sfh\right] \quad (6)$$

where, E_f = total fluid energy
$k_{eff,pm}$ = effective thermal conductivity of the medium
S_f^h = fluid enthalpy source term

Continuity equation

$$\frac{\partial u_i}{\partial x_i} = 0 \quad (7)$$

Momentum equation

$$u_j \frac{\partial u_i}{\partial x_j} = -\frac{1}{\rho}\frac{\partial p}{\partial x_i} + \frac{\partial}{\partial x_j}\left[(v + v_T)\left(\frac{\partial u_i}{\partial x_j} + \frac{\partial u_i}{\partial x_i}\right)\right] + \frac{f_j}{\rho} \quad (8)$$

Momentum equation for PM
Porous medium is modeled by the addition of a momentum source term to Eq. (8); the source term is:

$$S_i = \left(\sum_{j=1}^{2} D_{ij\mu v_j} + \sum_{j=1}^{2} C_{ij}\frac{1}{2}\rho|v|v_j\right) \quad (9)$$

where S_i is the source term for the i^{th} (*x* or *y*) momentum equation, $|v|$ is the magnitude of the velocity and *D* and *C* are prescribed matrices. This momentum sink contributes to the pressure gradient in the porous cell, creating a pressure drop that is proportional to the fluid velocity in the cell. The right-hand side of Eq. (9) is composed of two parts: a viscous loss term (Darcy, the first term), and an inertial loss term (second term).

Species transport equations
While solving the conservation equations for chemical species, the local mass fraction of each species, Y_i is predicted through the solution of a convection-diffusion equation for the i^{th} species. This conservation equation takes the following form:

$$\nabla.(\rho\bar{v}Y_i) = -\nabla.\bar{J}_i + R_i + S_i \quad (10)$$

where R_i is the net rate of production of species *I* by chemical reaction and S_i is the rate of creation by addition from the dispersed phase plus any user-defined sources. An equation of this form will be solved for *N*-1 species where *N* is the total number of fluid phase chemical species present in the system. In the current study a total of six species are considered.

NOx transport equation
The mass transport equation for the NO species is solved by taking into account convection, diffusion, production and consumption of NO and related species. For the thermal and prompt NOx mechanisms, only the NO species transport equation is needed:

$$\nabla.(\rho\bar{v}Y_{NO}) = \nabla.(\rho D\nabla Y_{NO}) + S_{NO} \quad (11)$$

Boundary conditions
The boundary conditions are; Inlet- Velocity inlet, mixture velocity = 0.9m/s; Outlet- Pressure outlet, pressure= atmospheric; Wall- Stationary wall, no slip.

Meshing and Simulation

The computational domain is built in GAMBIT 2.3.16, meshed using quad elements and exported to the FLUENT for simulation. Grid independence tests were conducted to arrive at the suitable grid size in each case. The meshed model is shown in Figure 2; T_2, T_3, T_4 and T_5 represent the temperatures at salient locations such as preheat layer, PM interface, surface of reaction layer and 2.5 cm above the top surface respectively. The first order upwind scheme is selected for discretization of the governing equations. Simulations are performed to study the effects of thickness and porosity of the reaction layer on the combustion performance of the PMB. Pure butane is assumed as fuel. The contours of temperature and NO_x formation are obtained in each case and compared, to find the optimum thickness and porosity of the reaction layer for a given preheat layer.

Figure 2. The meshed simulation model of PMB.

RESULTS AND DISCUSSION

Experimental Results

Selection of best PM configuration

First of all, by keeping the preheat layer fixed, the type and number of layers of reaction layers are varied. Table 1 shows the summary of trials made to find out the suitable PM configuration for the present study. It is seen that reaction layer with alumina foam of 8ppcm

yielded maximum flame temperature and minimum CO and NO_x emissions. Hence, this configuration is selected as the best.

Table 1. Summary of the trials on PMB.

Type of reaction layer	T_{max} (K)	Emission (ppm)	
		CO	NO_x
Alumina sphere, 20mm	878	352	4
Alumina sphere, 30mm	873	423	6
Alumina foam, 8 ppcm	1002	36	9
Alumina foam, 8 ppcm + Sphere,10mm	986	159	10
Alumina foam, 8 ppcm + Sphere,20mm	887	177	12
Alumina foam, 8 ppcm + Sphere,30mm	823	202	3

Temperature distribution

The transient temperature distribution within the burner including the inlet chamber is shown in Figure 3. T_1, T_2, T_3, T_4 and T_5 represent the temperatures at the inlet chamber, preheating layer, interface between two PM layers, top of reaction layer and 2.5 cm above the top surface respectively. The maximum temperature is observed at the surface (T_4) and maintained above 973K after reaching the steady state. This clearly indicates that the proposed burner operates in the surface stabilized combustion mode. The trend of T5 shows that the flame is extended sufficiently above the surface which is a desirable situation for practical cooking applications. The temperatures T_2 and T_3 never exceeded 523K. The temperature at the inlet chamber (T_1) is observed to be within 353K after a considerable period of operation, which rules out the possibility of a flash-back.

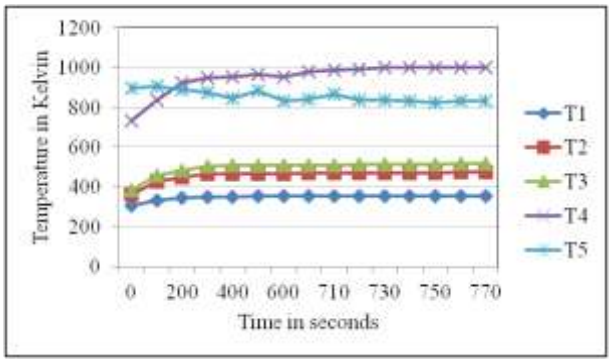

Figure 3. Transient temperature distribution within the PMB.

Emissions and combustion efficiency

Figure 4 shows the emission trends of CO, NOx and SO_2. During the testing period the CO emission has come to a steady value of around 30 ppm whereas NOx and SO_2 emissions are at 10 ppm and below. These values are well below the set limits of global emission norms. The combustion efficiency of the PMB is found to be fairly above 90% for an average excess air ratio of 1.8 and CO_2 emission of 8% vol. This indicates that fairly good combustion is occurred within the burner.

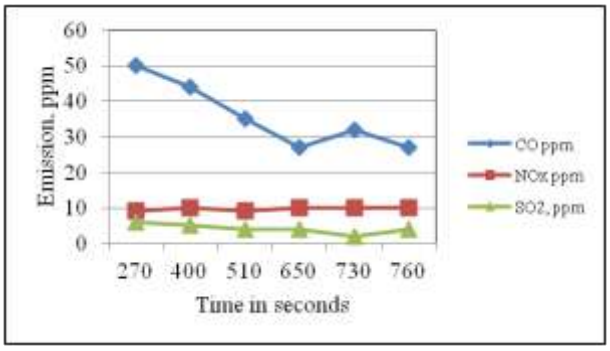

Figure 4. Emission characteristics of the PMB.

Comparison of PMB and CB

The performance characteristics of PMB and CB are compared in Table 2. It is observed that CB could not produce a sustainable flame in the premixed mode at any rates of fuel input. Hence we tested it without premixing, starting from 0.45lpm to the full flow (3lpm). It is interesting to note that at 0.45 lpm the flame produced by the CB was very weak with a maximum temperature of only 815K whereas the PMB could produce an excellent flame of 1002K which is even higher than the maximum flame temperature (981K) for CB at the full fuel input of 3 lpm. It is also worth noting that the average NOx formation above 973K in the PMB is only 10 ppm whereas for the CB it is 38 - 41 ppm; the CO emission (36 ppm) is well within the acceptable limit. Hence it can be concluded that the proposed PMB with a fuel input of 0.45lpm is compatible with the CB with full fuel input of 3 lpm, at the same time reducing the NOx significantly. The thermal efficiency is improved by 51% compared to CB, for the same thermal load. Jugjai and Rungsimuntuchart (2002) had proposed a heat re-circulating, PM domestic burner for which they claimed 50% saving in energy. It was a combination of CB and PM with LPG as fuel.

Table 2. Comparison of PMB and CB.

Characteristic	PMB	CB			
	0.45 lpm	0.45 lpm	1 lpm	2 lpm	3 lpm
T_{max}, K	1002	815	932	973	981
η_h	71	47	33	27	27
NOx, ppm	10	5	29	38	41
CO, ppm	36	118	4	2	2

Simulation Results

Grid independence test

The computational model was initially meshed with 15402 unstructured quad cells and simulated for combustion in the PM. The model was then improved

by gradient adaptation technique by refining large cells that displayed high velocity gradients, where a model with a higher cell count was produced. This process was repeated, each time producing a model with a higher cell count than the previous model. Subsequently five models were produced with 22491, 80715, 164622, 166134 and 166161 cells respectively. As shown in Figure 5, the surface temperature (T_4) converged as the mesh resolution approached 80715 cells; this mesh size which was chosen to determine the NO_x emission.

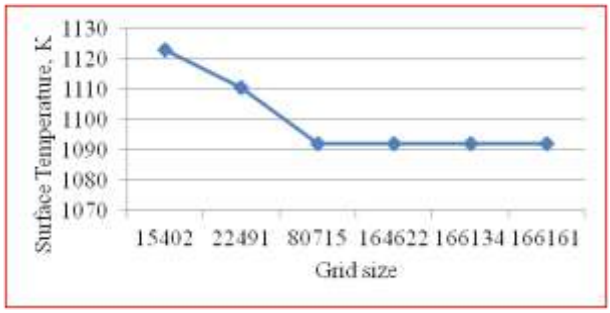

Figure 5. Grid size versus surface temperature.

Effect of thickness of reaction layer

The summary of predicted temperatures at the salient points (as defined in Figure 2) and the NO_x emissions for various thicknesses of reaction layer is provided in Table 3. It shows that, considering 12.7mm as the base case, a decrease in thickness could yield higher combustion temperatures but there is a possibility for the preheat layer getting heated more (as evidenced by the value of T_2 = 382 K which is the maximum compared to the other cases) which may cause serious flash-back; this situation puts restriction on the reduction of thickness. When the thickness is increased to 17mm, temperature is again increased compared to the base case. In this case, the problem of overheating of the preheat layer is eliminated. When the NO_x emission pattern is considered, the thickness must be compromised at 12.7mm, as it has the minimum emission. Thus Case 2 is apparent to be the best.

Table 3. Effect of thickness of reaction layer on temperature and NO_x predictions of PMB

Case	Thickness (mm)	Temperature in K				NO_x ppm
		T_2	T_3	T_4	T_5	
1	7.0	382	627	1362	1443	35.12
2	12.7	361	482	1148	1269	13.5
3	17.0	300	381	1353	1433	21.7

Effect of porosity of reaction layer

The summary of predicted temperatures at the salient points and the NO_x emissions for various porosities of reaction layer is provided in Table 4. It is very clear that the Case 3 has the maximum surface temperature and minimum NO_x emission. So from these two simulations, it may be concluded that, the reaction layer of thickness 12.7mm and porosity 84% is the optimum choice for the PMB; this prediction conforms well with the experimental result which also shows that PMB with one reaction layer of thickness 12.7mm and porosity 84% is the best. The temperature and NO_x emission profiles of the optimum PM configuration are shown in Figures 6 and 7.

Table 4. Effect of porosity of reaction layer on temperature and NO_x predictions of PMB

Case	Porosity (%)	Temperature in K				NO_x ppm
		T_2	T_3	T_4	T_5	
1	60	362	549	860	1108	17.8
2	70	363	488	865	1116	21.35
3	84	361	482	1148	1269	13.5
4	90	300	364	877	1133	30.85

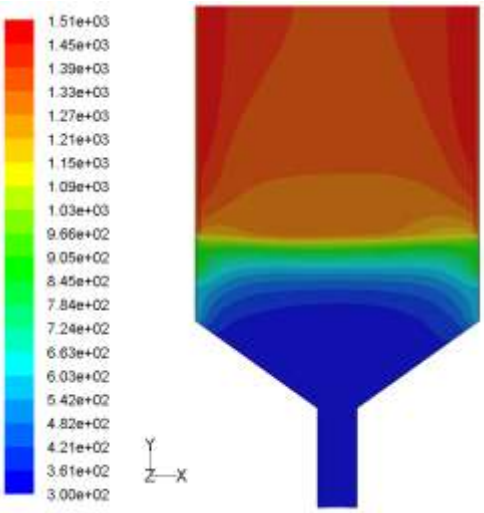

Figure 6. Temperature profile for PMB with reaction layer thickness 12.7mm and porosity 84%.

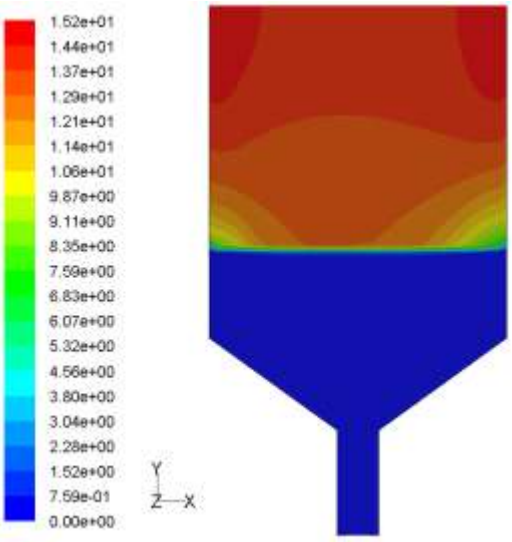

Figure 7. NO_x emission profile of PMB with reaction layer thickness 12.7mm and porosity 84%.

Comparison of simulation and experimental results

The axial temperature distribution along the central axis within the PMB is shown in Figure 8. It is observed T_4 is about 1147 K which is slightly higher than the

experimental value (1002K). The over-prediction is attributed to the use of one-temperature model with single-step reaction, as also observed by Zhou and Pereira (1998). However, unlike the experimental observation, the temperature downstream of the PM layers is increasing; this is due to the assumption of negligible heat loss through the walls. The temperatures at the centre of preheating layer (T_2) and the interface of the PM layers (T_3) are also highlighted. The predicted values of T_2 and T_3 (361 K and 482 K respectively) are less than the experimental values (474 K and 519K respectively). This under-prediction is due to the fact that the heat feed-back upstream by radiation from the reaction zone has not been incorporated in the model; therefore conduction through the PM matrix becomes the only mode for the heat feed-back. The average NO_x is estimated to be about 13.5 ppm, which is slightly higher than the experimental value (10ppm). This discrepancy is due to the weakness of the one-step reaction model to make realistic prediction of emission (Zhou and Pereira, 1998); however the error is within the acceptable range. Moreover, the one temperature model with single step reaction used in this simulation could not predict the formation of CO, which is possible by means of multi-step reaction models. In order to account multi-step kinetics and to allow the gas and solid phases have own temperatures, user-defined functions and scalars are to be implemented and incorporated into the FLUENT (Shi et al., 2008) which has recently gained attraction to handle PMC problems.

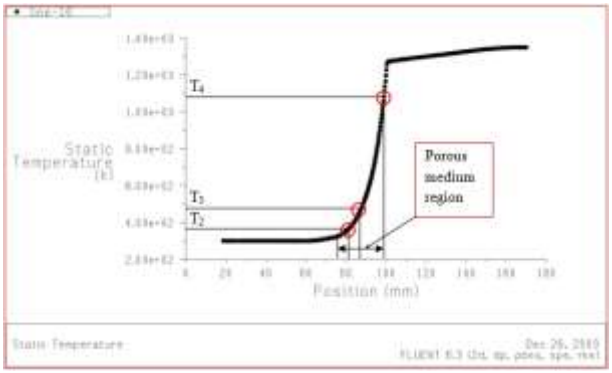

Figure 8. The predicted axial temperature distribution inside the PMB.

CONCLUSION

A user-friendly, premixed, PM surface burner for domestic applications is developed successfully and tested for its combustion and emission characteristics. The study was purely on practical grounds so as to compare its benefits with the CB. It is observed that the proposed PMB is capable to achieve 51 % improvement in thermal efficiency with significant reduction in NOx (10 ppm) compared to the CB (38 - 41 ppm). Hopefully, the current study would open doors for realizing energy efficient household burners using PMC technology. More experiments may be done on variety of fuels, number of PM layers and other PM geometries (cylindrical and spherical). The 2D simulation performed on the PMB model could yield satisfactory predictions; however, the scope for a 3D simulation incorporating detailed reaction kinetics, thermal non-equilibrium between gas and solid phases, and radiation is obvious.

ACKNOWLEDGEMENT

The authors would like to thank the Ministry of Technology and Innovation, Malaysia and Universiti Sains Malaysia for the financial support for this research work.

REFERENCES

Bone, W. A., 1912, Surface combustion, *The Journal of the Franklin Institute*,173, 2, 101-131.

Bouma P. H., Eggels R. L. and Goey L. P., Nieuwenhuizen, J. K., Drift, A. V., 1995, A numerical and experimental study of NO-emission of ceramic foam surface burners, *Combust. Sd. Technol.*, 108, 193-203.

Hanamura K. and Echigo R., 1991, An analysis of flame stabilization mechanism in radiation burners, *Wfirme- und Stoffiibertragung*, 26, 377-383.

Hays J. W., 1933, Surface Combustion Process, *US Patent No. 2095065*.

Jugjai S. and Rungsimuntuchart N., 2002, High efficiency heat-recirculating domestic gas burners, *Experimental Thermal and fluid Science*, 26, 581-592.

Jugjai S., Sawananon A., 2004, The surface combustor-heater with cyclic flow reversal combustion embedded with water tube bank. *Fuel*, 83, 2369–2379.

Lammers F.A. and de Goey L.P.H., 2003, A numerical study of flash back of laminar premixed flames in ceramic-foam surface burners, *Combustion and Flame*, 133, 47–61.

Lucke C. E., 1913, Design of surface combustion appliances, *The Journal of Industrial and Engineering Chemistry*, 5, 10, 801-824.

Marbach T. and Agrawal A. K., 2005, Experimental study of surface and interior combustion using composite porous inert media, *Journal of Engineering for Gas Turbines and Power*, 127, 307–313.

Marbach T. L., Sadasivuni V. and Agrawal A. K., 2007, Investigation of a miniature combustor using porous media surface stabilized flame, *Combustion Science and Technology*, 179, 9, 1901 – 1922.

Mujeebu M. A., Abdullah M. Z., Abu Bakar M. Z., Muhad R. M. N. and Khalil M., 2009a, Combustion in Porous media and its applications- A comprehensive survey, *Journal of Environmental Management*, 90, 2287–2312.

Mujeebu M. A., Abdullah M. Z., Abu Bakar M. Z. and Khalil M., 2009b, Applications of porous media combustion technology- A review, *Applied Energy*, 86, 9, 1365–1375.

Nakamura Y., Itaya Y., Miyoshi K. and Hasatani M., 1993, Mechanism of methane-air combustion on the surface of a porous ceramic plate, *J. Chem. Eng. Jpn.*, 26, 2, 205-211.

Nemoda S., Trimis D. and Goran, 2004, Numerical simulation of porous burners and hole plate surface burners, *Thermal Science*, 8, 1, 3-17.

Shi J.R., Xie M.Z., Liu H., Li G. and Zhou L., 2008, Numerical simulation and theoretical analysis of premixed low-velocity filtration combustion, *International Journal of Heat and Mass Transfer*, 51, 7-8, 1818-1829.

Taylor J.R., 1997, *An Introduction to Error Analysis: The Study of Uncertainties in Physical Measurements*. (Second Edition), University Science Books, Sausalito, CA 94965.

Williams A., Woolley R. and Lawes M., 1992, The formation of NO_x in surface burners, *Combust. Flame*, 89, 157-166.

Zhou X. Y. and Pereira J.C.F., 1998, Comparison of four combustion models for simulating the premixed combustion in inert porous media, *Fire and Materials*, 22, 5, 187–197.